DYNAMIC ANALYSIS OF DAMAGED MASONRY BUILDING REPAIRED WITH THE FLEXIBLE JOINT METHOD

A. KWIECIEŃ[1], P. KUBOŃ[1]

The paper presents a dynamic analysis of the damaged masonry building repaired with the *Flexible Joint Method*. Numerical analysis helped to determine the effect of the applied repairing method on natural frequencies as well as values of stresses and accelerations in the analyzed variants of numerical model. They confirmed efficiency of the proposed repair method.

Key words: polymer flexible joint, dynamic analysis, numerical modeling, dynamic resistance.

1. INTRODUCTION

Polymer flexible joints that have been used in repairing of damaged masonry buildings [1], have also showed high resistance to the strong dynamic influences, which was confirmed during *in situ* investigations [2], [3]. Those investigations allowed identifying elastic parameters (Young's modulus) of the analyzed masonry building, estimated for different stages: undamaged, damaged and repaired using the *Flexible Joint Method*. These parameters were then included in the FEM model, which was subjected to the strong ground motion. Comparison of the dynamic response of analyzed masonry building in different stages is the main aim of this paper.

2. DESCRIPTION OF THE ANALYZED BUILDING

A subject of conduced analysis was the storied, masonry building of the transformer station (Fig. 1). The building was constructed on a rectangular plan with the external walls dimensions of 4.42[m]×3.07[m] and the height of 2.90[m] in the roof base and of 3.44[m] in the roof ridge. Walls of the building were constructed in the traditional technology, made of brick on cement-lime mortar with thickness of 25[cm], covered with a thin layer of plaster and based on a concrete floor plate with a thickness of 30[cm], which was constructed on the brick benches buried in the ground at 1.6[m].

[1] Cracow University of Technology, Department of Civil Engineering, Kraków, Poland, e-mail: pkubon@pk.edu.pl

The building was covered with a pitched roof made of reinforced concrete plate with a thickness of 10[cm].

Fig. 1. View of the analyzed building – undamaged stage.
Rys. 1. Widok badanego budynku – stan nieuszkodzony

Next, the building was damaged by hitting excavator bucket in the rear upper corner at ceiling level, which generated a torsion vibration mode and caused formation of cracks in the plane of the walls (Fig. 2). A map of created damages was more or less characteristic for masonry buildings located in seismically active areas, obtained after an earthquake. The analyzed building was weakened to such extent that any small dynamic excitation could lead to its collapse, which was a positive factor from the research point of view.

Fig. 2. View of the analyzed building – damaged stage.
Rys. 2. Widok rozważanego budynku – stan uszkodzony

Subsequently, the building was repaired by cleaning and priming cracks and then filling in the largest ones with pieces of brick. Surfaces of the cracks were covered outside with a layer of gypsum and then cracks were filled in with polymer (pm/45)

dispensed under low pressure. Revision openings, made in the repaired cracks for the control, showed that the used polymer has well-filled empty spaces in the wall (Fig. 3).
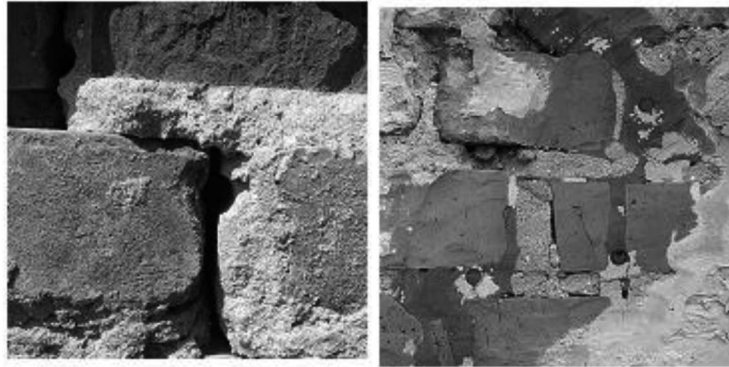
Fig. 3. Exemplary wall gaps and the final stage of its repair.
Rys. 3. Przykładowe szczeliny w murze oraz etap końcowy naprawy pęknięcia

After the repair, the building was subjected to strong dynamic excitation at soil surface [2, 3] with its resonance frequencies, what is dangerous for the structure [4]. There were no new cracks, what indicates that flexible polymer joint restore coherence of the cracked walls (Fig. 4).

Fig. 4. View of the repaired building during the strong dynamic excitation.
Rys. 4. Widok naprawionego budynku w trakcie silnego wzbudzenia dynamicznego

3. Estimation of dynamic characteristics of the analyzed building

In order to estimate dynamic characteristics of the analyzed building, dynamic studies were performed for three different stages of the object. In the first, the undamaged building was studied, in the second the damaged one and finally the repaired one using

of polymer. Dynamic testing excitations were applied with the modal hammer PCB 086D50 and with the *Wibrosejs Mark IV*, which executed harmonic vertical vibrations as well as impulse excitations on the soil surface at the distance of 15 m from the building [2, 3]. All vibrations were recorded by accelerometers arranged throughout the building (Fig. 5).
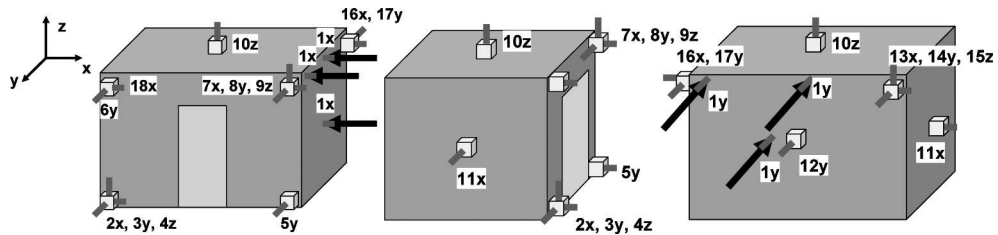
Fig. 5. Layout and description of the accelerometers – excitation with modal hammer.
Rys. 5. Rozkład oraz oznaczenie akcelerometrów – wymuszenie młotkiem modalnym

3.1. Resonant frequencies of analyzed building

Estimation of the inertance module was necessary, in order to determine resonant frequencies of three stages of the analyzed building. The accelerometer "8y", placed in the top corner of the front wall (Fig. 5), was assumed as a reference point for measurements. This accelerometer registered horizontal vibrations. Data received on this measuring point allowed identifying bending and torsion vibration forms in the plane of the building walls, which are the most sensitive to stiffness changes. The exemplary FFT plots for "8y" accelerometer for different building stages, in the case of the modal hammer hitting in the corner of the rear wall, are plotted in Fig. 6.

Subsequently, the inertance module was determined [5] by the equation (3.1):

$$(3.1) \qquad |I(\omega)| = \frac{\left|\ddot{X}(\omega)\right|}{|F(\omega)|}$$

Where:

$\left|\ddot{X}(\omega)\right|$ − amplitude-frequency acceleration characteristics (FFT) [(cm/s2)/Hz]
$|F(\omega)|$ − amplitude-frequency excitation force characteristics (FFT) [N/Hz]

Exemplary amplitude-frequency characteristic for dynamic excitation using modal hammer are presented in Fig. 7.

After the damage, the frequency response of the building has noticeably shifted towards lower frequencies, whereas repairing with polymer of the damaged structure has moved the mentioned response towards higher frequencies. Shifts scale for higher frequencies is greater than for lower ones. This trend can be observed both in the FFT as well as in the inertance module charts (Fig. 6, Fig. 8.).
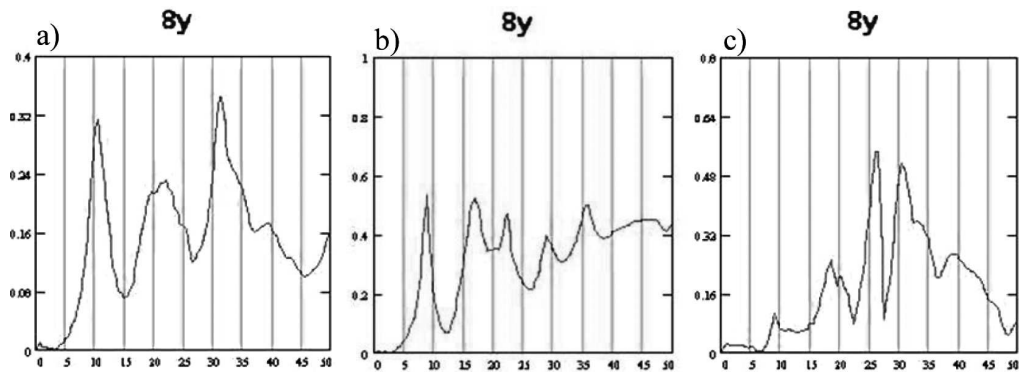
Fig. 6. Exemplary FFT plots for the building (in different scale): a) undamaged, b) damaged, c) repaired.
Rys. 6. Przykładowe wykresy FFT dla budynku (różna skala): a) nieuszkodzonego, b) uszkodzonego,
c) naprawionego
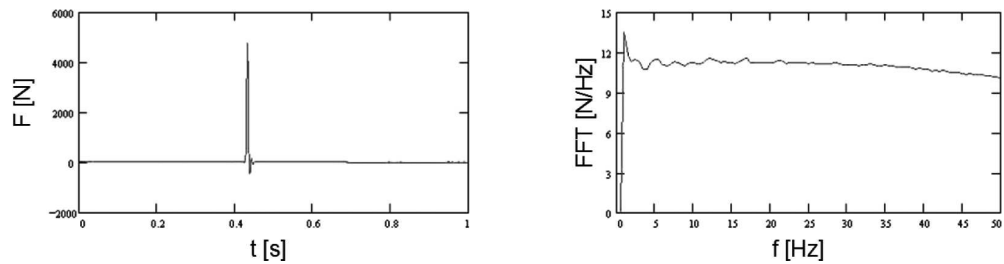
Fig. 7. Acceleration chart for modal hammer excitation and corresponding FFT.
Rys. 7. Przebieg czasowy wymuszenia młotkiem modalnym oraz odpowiadające mu FFT
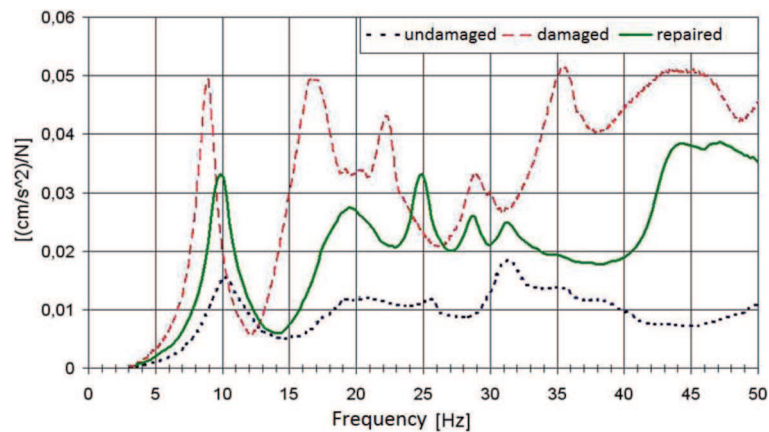
Fig. 8. Changes of the inertance module $|I(f)|$ of the analyzed building, recorded on the sensor 8y.
Rys. 8. Zmiany modułu inertancji $|I(f)|$ badanego budynku, zarejestrowane na czujniku 8y

Shown in the amplitude-frequency characteristics of the inertance (Fig. 8), estimated for the "8y" measuring point of the building being in three stages, illustrate the influence of damage and repair for the dynamic response of the building. The inertance amplitudes increase significantly after cracking in relation to the undamaged building and after cracks repairing with polymer they are reduced again. Analysis of the inertance functions allowed determining changes in resonant frequency at different stages of analyzed building, which are presented in Table 1.

Table 1

Resonant frequencies for different stages of analyzed building.
Częstotliwości rezonansowe analizowanego budynku w różnych jego stanach

Resonant frequencies f [Hz] (change in %)			
Building stage	I resonant	II resonant	III resonant
Undamaged	10,27 (100%)	20,30 (100%)	31,58 (100%)
Damaged	8,92 (87%)	16,79 (83%)	22,32 (71%)
Repaired	9,84 (96%)	19,67 (97%)	24,94 (79%)

The compliance module $|A(\omega)|$ [m/N] is related [5] to the inertance module $|I(\omega)|$ [(m/s^2)/N] in frequency field ω by the relation (3.2). As in the inertance case (Fig. 8.), the compliance estimated for "8y" measuring point confirms influence of damage and repair for the dynamic response of the building (Fig. 9).

$$(3.2) \qquad |A(\omega)| = \frac{|I(\omega)|}{\omega^2}$$
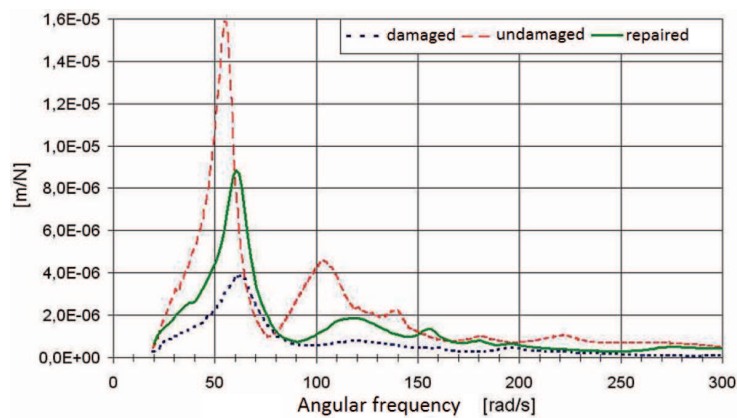
Fig. 9. Changes of compliance module $|A(\omega)|$ of the analyzed building, recorded on the sensor 8y.
Rys. 9. Zmiany modułu inertancji $|A(\omega)|$ badanego budynku, zarejestrowane na czujniku 8y

3.2. Damping parameters

One of the damping measures [6], which could be estimated in dynamic investigations *in situ*, is the logarithmic decrement δ, which could be defined as natural logarithm of quotients of consecutive amplitudes [7] and is associated with a fraction of critical damping ξ by (3.3).

$$(3.3) \qquad \delta = \ln \frac{A_i}{A_{i+1}} = \frac{2\pi\xi}{\sqrt{1 - \xi^2}}$$

The critical damping fraction can be estimated using the "half power bandwidth" method, which requires the compliance characteristics (Fig. 9) in vicinity of resonant frequency. It involves the frequencies ω_1 and ω_2 corresponding to the amplitude $0.707A_{max}$, which are determined from the compliance curves (A_{max} is the maximum amplitude at the compliance curve). Thus, the critical damping fractions for three resonant frequencies of the building in three stages are determined based on formula (3.4). The logarithmic decrement was estimated due to relation (3.3). Obtained values of damping parameters are presented in Table 2.

Table 2

Critical damping ratio and logarithmic decrement for different stages of analyzed building.
Ułamek tłumienia krytycznego oraz logarytmiczny dekrement tłumienia dla różnych stanów budynku

Critical damping ratio ξ [-] (estimated using "half power bandwidth" method)			
Building stage	I resonant	II resonant	III resonant
Undamaged	0,230 (100%)	0,138 (100%)	0,113 (100%)
Damaged	0,143 (62%)	0,072 (52%)	0,063 (56%)
Repaired	0,166 (72%)	0,084 (61%)	0,068 (60%)
Logarithmic decrement δ [-]			
Building stage	I resonant	II resonant	III resonant
Undamaged	1,485 (100%)	0,934 (100%)	0,714 (100%)
Damaged	0,971 (62%)	0,453 (52%)	0,397 (56%)
Repaired	1,058 (72%)	0,625 (72%)	0,068 (60%)

$$(3.4) \qquad \xi = \frac{\Delta\omega}{2\omega_r}$$

$$(3.5) \qquad \xi_i = \frac{\alpha}{2\omega_i} + \frac{\beta\omega_i}{2}$$

where:

$\Delta\omega = \omega_2 - \omega_1$ − width of the compliance characteristics chart measured at the level of *0.707 A_{max}* [rad/s]

ω_r – resonant frequency of the compliance characteristics [rad/s]

α, β – Rayleigh parameters of the damping model (5.1)

Damping coefficients ξ for the second dominant resonant frequency were calculated from the first and the third dominant resonant frequencies according to equation (3.5), using the equivalent Rayleigh damping method (Fig. 10). Comparison of estimated damping parameters shows that damage of the building reduces them by almost half, while repairing cracks with polymer causes growth of damping by about 10% in comparison to the undamaged building (Fig. 10).
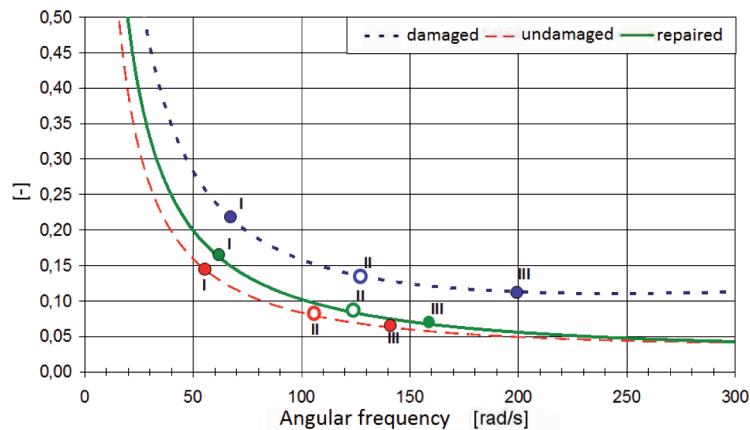
Fig. 10. Function of critical damping fraction determined for three stages of the building.
Rys. 10. Funkcja ułamka tłumienia krytycznego wyznaczone dla trzech faz pracy budynku

4. Numerical identification of elastic parameters of the analyzed masonry building

The FEM model of the repaired building was constructed on the basis of the laser gravimetric maps, which allowed determining the grids of points. These grids defined walls of the building model in the *MSC MARC* system, considering the actual scheme of cracks filled with polymer – marked with white lines in Fig. 11.

The walls, the floor and the ceiling plate were modeled by shell elements whereas the ceiling rib by beam elements. Elastic fixing in the soil was modeled as a system of horizontal and vertical springs. There were determined 11 natural frequencies (Table 3) of the FEM models for the three stages of the building: undamaged, damaged and repaired. In the first approach undamaged building was analyzed. On the basis of experimentally identified dynamic characteristics of the structure (modal hammer test) elasticity of the soil were estimated as well as parameters of linear-elastic material – masonry walls and concrete elements.
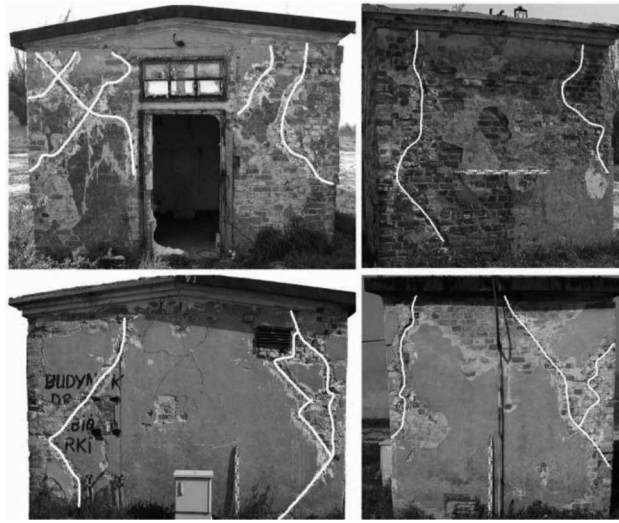
Fig. 11. Location of the repaired cracks in the building by the laser gravimetric determination.
Rys. 11. Lokalizacja sklejonych pęknięć w budynku przy użyciu grawimetrii laserowej

Table 3

Free vibrations obtained numerically and from measurements (in brackets).
Drgania własne otrzymane z analiz numerycznych oraz pomiaru (wartości w nawiasach)

Form of vibration	Free vibrations [Hz] – numerically (measurements)		
	Undamaged	Damaged	Repaired
I (I resonant)	**10,27 (10,27)**	**9,18 (8,92)**	**9,92 (9,84)**
II	10,91	9,31	10,45
III	15,06	14,68	15,00
IV (II resonant)	**20,40 (20,30)**	**16,38 (16,79)**	**19,30 (19,67)**
V	24,14	20,29	23,21
VI	25,49	21,70	24,24
VII	27,52	22,62	25,00
VIII (III resonant)	**31,03 (31,58)**	**25,17 (22,32)**	**29,87 (24,94)**
IX	32,42	26,46	30,28
X	35,06	27,49	31,86
XI	36,04	27,97	32,64

Values of the model parameters in the case of masonry walls were: E = 1.4 [GPa], $v = 0.2$ i $\rho = 1700$ [kg/m^3], whereas in the case of the concrete elements: E = 30 [GPa], $v = 0.17$ and $\rho = 2400$ [kg/m^3]. In this model, the elastic properties of the joints were identical with the properties of the brick walls. The applied numerical model reflects relatively well the dynamic behavior of the real undamaged object, that is practically all three identified resonant frequencies are within the margin of 2% error (Table 3).

In the next approach, dynamic stiffness of the joints adopted as a crack unfilled with polymer was identified. All model parameters were left as in the model of the undamaged construction, apart from joints stiffness adjusted on the basis of the dynamic response of the building. Finally, this parameter was set at $E = 3$ [MPa]. The numerical model of the damaged building yielded (in a satisfactory manner) dynamic behavior of the real structure, since first two identified resonant frequencies were within the margin of 3% error, while third one was adjusted within the margin of 12% error (Table 3).

In the last approach, the dynamic stiffness of the flexible joints was identified. This joint was assumed as the crack filled in with injected polymer. As previously, the model parameters were left as in the model of the undamaged building, apart from joint stiffness adjusted on the basis of dynamic response of the repaired building. Finally, this parameter was set at $E = 50$ [MPa]. Also in this case applied numerical model of the repaired building yielded quite good agreement with the real structure. The first two identified resonant frequencies were within the margin of 2% error, while third one differed significantly within the margin of 20% error (Table 3).

5. Estimation of dynamic resistance

In order to estimate dynamic resistance of the analyzed masonry building, simplified model of the building was built in the *ABAQUS FEA* system [8]. It was a modification of the previously analyzed model, where soil structure interaction has been taken into account, and which was used to identify elastic parameters of the analyzed construction elements (walls, elements describing cracks and flexible polymer joints. Simplification of the new model was based on replacing the soil elastic supports by the rigid foundation. The aim of the simplification was to compare only the dynamic response of the upper part of the building (over the foundation), considered for three stages of the working masonry system.
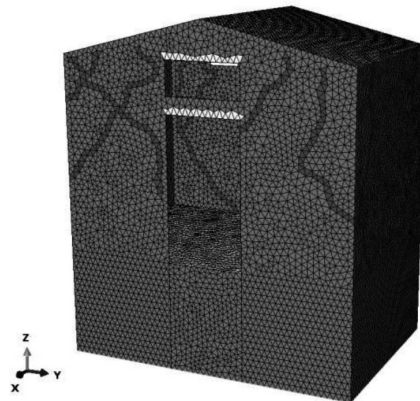
Fig. 12. FEM model of analyzed building in the ABAQUS system.
Rys. 12. Podział modelu na elementy skończone w programie ABAQUS
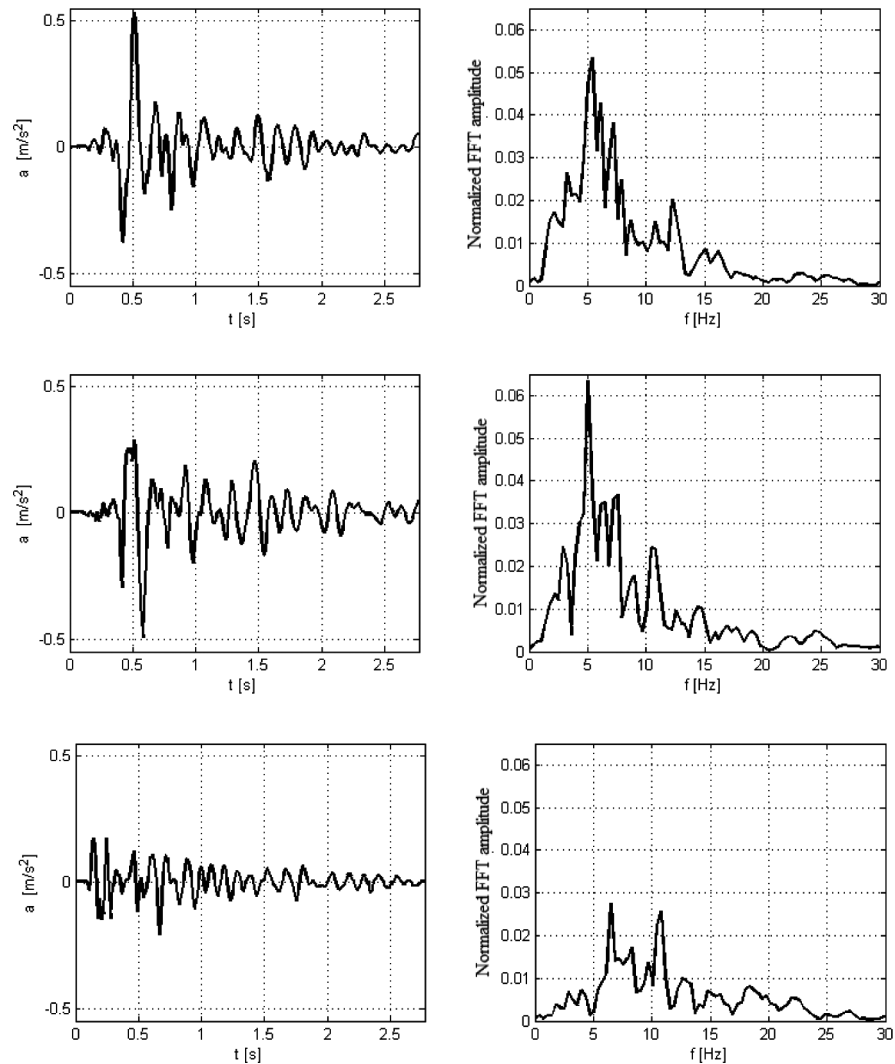
Fig. 13. Horizontal (a_x, a_y) and vertical (a_z) components of kinematic excitation along with corresponding FFT.

Rys. 13. Składowe pozioma (a_x, a_y) oraz pionowa (a_z) wymuszenia kinematycznego wraz z odpowiadającymi im transformatami FFT

The simplified FEM model (Fig. 12) consisted of more than 25 thousand shell-type (S3R) and beam (B31) type finite elements. Division of the model into finite elements with an indication of cracks is shown in Fig. 12. The numerical analysis included free vibrations estimation, and kinematic load implemented through the forced movement of the basement as a rigid body – without taking into account soil-structure interaction. Mining tremor registered on the LGOM (*Legnicko-Głogowski Okręg Miedziowy*)

area has been assumed as the kinematic excitation. Acceleration components (in three mutually perpendicular directions) were applied directly to the rigid solid foundation, without taking into account vibrations reduction resulting from the soil-structure interaction. Kinematic excitation in a horizontal (a_x, a_y) and vertical (a_z) directions, together with the corresponding Fourier transforms, are shown in Fig. 13.

Three variants of the simplified FEM model were considered: the undamaged building, the cracked building and the repaired one with flexible polymer joint. As calculation results, first five natural frequencies of the analyzed construction as well as maximum values of stresses and accelerations in selected points of the structure were obtained (Fig. 14).
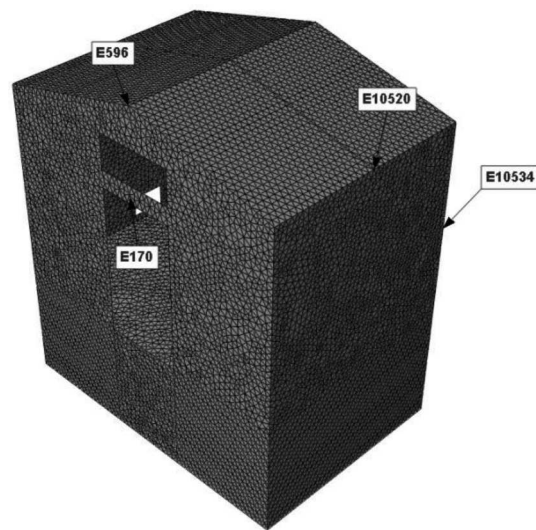
Fig. 14. Points selected for analysis of stress and resultant acceleration.
Rys. 14. Punkty wybrane do analizy naprężeń oraz wypadkowych przyspieszeń

Table 4

Resonant frequencies for different stages of the analyzed building – the simplified model.
Częstotliwości rezonansowe dla różnych stanów analizowanego budynku – model uproszczony

Building stage	Undamaged	Damaged	Repaired
$f1$[Hz]	18.9* (100%)	12.3* (65%)	16.5* (87%)
$f2$[Hz]	20.3* (100%)	13.5* (66%)	17.1* (84%)
$f3$[Hz]	25.5* (100%)	17.7* (69%)	22.6* (89%)
$f4$[Hz]	30.5** (100%)	19.2** (63%)	25.5** (84%)
$f5$[Hz]	30.7** (100%)	20.7** (67%)	26.7** (87%)

* bending vibrations, ** torsion vibrations

First five natural frequencies obtained for different variants of the simplified model are presented in Table 4. Comparison of the results obtained for the models of the undamaged and cracked building showed decrease of the calculated natural frequencies in the range of 31÷37%. In the case of the repaired building model the frequencies increased in the range of 26÷34% in comparison to the damaged one.

Simultaneously, there was no change observed in the nature of vibrations (torsion, bending vibrations). Exemplary forms of free vibrations obtaining for analyzed three FEM model variants are shown in Fig. 15.
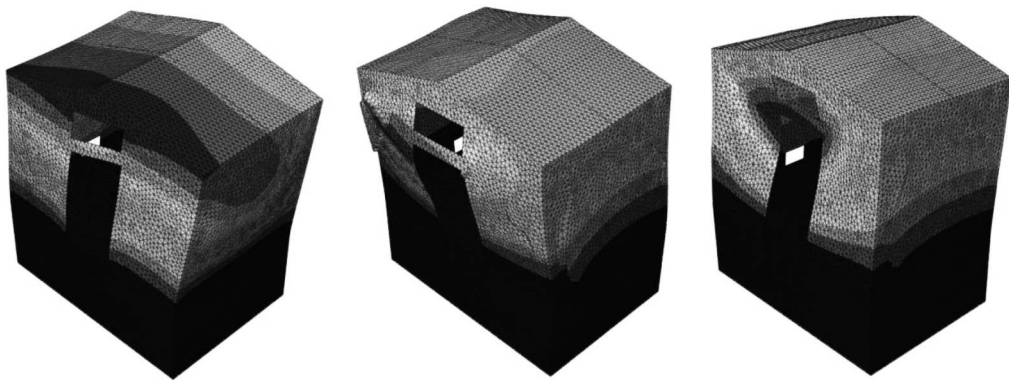
Fig. 15. Second free vibrations forms: a) undamaged building $f_2 = 20.35\ [Hz]$, b) damaged building $f_2 = 13.5\ [Hz]$, c) repaired building $f_2 = 17.1\ [Hz]$.
Rys. 15. Druga postać drgań własnych: a) budynek nieuszkodzony $f_2 = 20.35[Hz]$, b) budynek uszkodzony $f_2 = 13.5[Hz]$, c) budynek naprawiony $f_2 = 17.1[Hz]$

The dynamic analysis of the simplified model was performed including kinematic load (Fig. 13) acting at the model support. The damping model defined by the relation (5.1) was applied, where the pars of the Rayleigh parameters α and β were determined according to the equation (3.5) and Fig. 10. In the determination process, the values of the damping coefficients ξ_i (in the range of 0.230÷0.063) were taken for calculation from Table 2. The calculated values of the parameters α and β were presented in Table 5.

$$(5.1) \qquad\qquad [C] = \alpha\,[M] + \beta\,[K]$$

where:

C – damping matrix, M – mass matrix, K – stiffness matrix.

Data included in Table 5 shows that in the case of the analyzed construction the mass damping plays dominant role. In the case of the damaged building, stiffness damping is very low and do not exceed 5% of analogical parameter for undamaged construction.

Calculated α and β parameters of the Rayleigh damping model.
Parametry α i β wyznaczone dla modelu tłumienia wg Rayleigh'a

Building stage	Undamaged	Damaged	Repaired
α	3,260 (100%)	2,358 (72%)	3,081 (94%)
β	0,020 (100%)	$9.605*10^{-4}$ (5%)	$2.175*10^{-3}$ (11%)

Horizontal accelerations a_x [m/s^2] with corresponding FFT transforms of the excitation and the building responses in three different stages (determined in the E595 point) are shown in Fig. 16. It is observed that undamaged building responses with the excitation characteristic as the stiff body and after the damage process the dynamic response increases considerably (many times) with particular resonant frequencies. This is the reason why cracked masonry buildings are vulnerable to after-shock excitations in seismic areas. Repair of the cracks with polymer flexible joints decreases this response, shifting them to the higher frequency band.

Maximum values of stress and accelerations determined in selected points of the analyzed building are shown in Tables 6 and 7. These results confirm that the building damage increases dynamic response and stress level, whereas repairing using of polymer flexible joints causes decreasing of these values. The presented results indicate that the presented repair method is dynamically very efficient.

Table 6

Maximum values of stress in selected elements [kPa].
Maksymalne wartości naprężeń [kPa] dla wybranych elementów

Building stage	Undamaged	Damaged	Repaired
E(170)	1,85 (100%)	3,58 (193%)	2,97 (160%)
E(596)	5,54 (100%)	21,50 (388%)	13,34 (241%)
E(10520)	3,12 (100%)	9,79 (314%)	5,74 (184%)
E(10534)	5,19 (100%)	27,54 (531%)	15,85 (305%)

Table 7

Maximum values of horizontal accelerations in selected points [m/s^2].
Maksymalne wartości poziomych przyspieszeń [m/s^2] w wybranych punktach

Building stage	Undamaged	Damaged	Repaired
E(170)	0,57 (100%)	0,92 (161%)	0,82 (144%)
E(596)	0,58 (100%)	0,95 (164%)	0,95 (164%)
E(10520)	0,58 (100%)	0,83 (143%)	0,61 (105%)
E(10534)	0,56 (100%)	0,67 (120%)	0,61(109%)
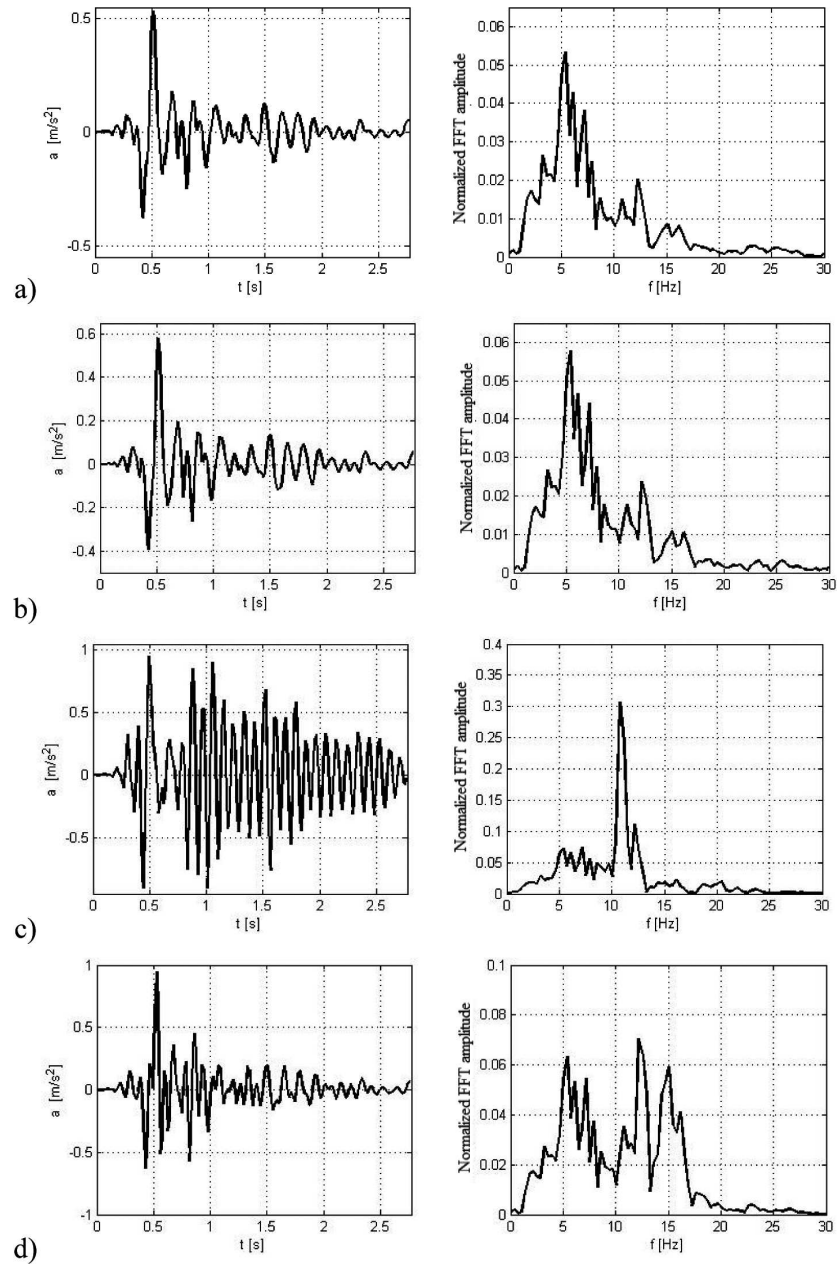
Fig. 16. Horizontal accelerations a_x [m/s^2] with corresponding FFT: a) excitation at the support, b) point E595 – undamaged, c) point E595 – damaged, d) point E595 – repaired.

Rys. 16. Przyspieszenia poziome a_x [m/s^2] z odpowiadającymi im FFT: a) wymuszenie u podstawy, b) punkt E595 – nieuszkodzony, c) punkt E595 – uszkodzony, d) punkt E595 – naprawiony

6. Conclusions

Presented dynamic investigations on the masonry building tested in situ, using of various dynamic excitations, allowed showing how changes the dynamic response of the undamaged, damaged and repaired masonry building. The examined dynamically innovative repair method, named the Flexible Joint Method (FJM), uses polymer flexible joints constructed in places of cracks by filling them with specially chosen polymer mass. Basing on the results of dynamic tests, carried out for three stages of the masonry building, two kinds of the FEM models were performed. Using the first one made in the MARC system, the material properties of the model were found. The next model built in the ABAQUS system put these parameters to use and allowed finding and comparing the dynamic responses of the undamaged, damaged and repaired masonry building excited by the mining tremor. The obtained results indicate the following conclusions:

1. Application of the flexible polymer joints during repairing damaged masonry building has improved the dynamic resistance of the analyzed structure;
2. Polymer flexible joints can be used during repairing of masonry buildings located in areas being at risk of seismic or paraseismic activity (dynamic excitation);
3. Carried out simplified numerical analysis presented how changes dynamic response of the upper parts (over the foundation) of the analyzed masonry structure, which was in different technical condition.
4. The real dynamic response of the building, taking into account the soil-structure interaction, will be subjected to further analysis;
5. Using of polymer flexible joints in repairing of masonry buildings is an innovative approach and its implementing in the FEM modeling of engineering structures for the practice purpose is one of the first.

References

1. A. Kwiecień, B. Zając, *Repairing cracked masonry buildings using a Flexible Joint Method* [in Polish], Konferencja Naukowo-Techniczna, Awarie Budowlane'07, Szczecin-Międzyzdroje 2007.
2. A. Kwiecień, B. Zając, *Dynamic response of the cracked masonry building repaired with the Flexible Joint Method – an innovative earthquake protection*, 7th International Conference of EASD EURODYN'2008, Southampton 2008.
3. A. Kwiecień, B. Zając, *Work of a flexible polymer joint on the example of destructive testing of building* [in Polish], Czasopismo Techniczne, Budownictwo 2-B/2009, Zeszyt 9, ROK 106.
4. P. Hawryszków, M. Klasztorny, *Protection of suspension footbridges with tuned mass dampers against excessive resonant vertical vibrations caused by vandal pedestrian loads*, Archives of Civil Engineering, **53**, 4, 607-637, 2007.
5. J. Giergiel, T. Uhl, *Identification of dynamic systems*, PWN, Warszawa 1990.
6. M. Salamak, *Vibration damping identification maximizing adjustment to viscous model in civil structures,* Archives of Civil Engineering, **53**, 3, 497-518, 2007.

7. R. Ciesielski *et al.*, *Structural Mechanics. A computer approach*, Arkady, Warszawa 1992.
8. ABAQUS Analysis User's Manual, Vol. I–VI, http://baribal.cyf-kr.edu.pl:2080

ANALIZA DYNAMICZNA USZKODZONEGO MUROWANEGO BUDYNKU NAPRAWIONEGO
Z ZASTOSOWANIEM POLIMEROWEGO ZŁĄCZA PODATNEGO

S t r e s z c z e n i e

W pracy przedstawiono analizę dynamiczną uszkodzonego budynku murowego naprawionego z zastosowaniem polimerowego złącza podatnego. Zbudowane modele numeryczne budynku w trzech stanach (nieuszkodzonym, uszkodzonym i naprawionym), o parametrach materiałowych zidentyfikowanych dynamicznymi badaniami doświadczalnymi in situ, umożliwiły wykonanie obliczeń MES oraz przeprowadzenie analiz porównawczych. Porównane zostały zmiany odpowiedzi dynamicznej budynku w trzech stanach na wymuszenie wstrząsem górniczym bez uwzględnienia interakcji z podłożem. Uzyskane wyniki potwierdziły skuteczność polimerowych złączy podatnych, jako sposobu naprawy pękniętych budynków murowanych na terenach sejsmicznych oraz tam, gdzie obiekty budowlane poddane są destrukcyjnym wymuszeniom parasejsmicznym.